Journal of Superconductivity and Novel Magnetism (2021) 34:243–249
https://doi.org/10.1007/s10948-020-05739-0

ORIGINAL PAPER

Magnetocaloric and Refrigeration Characteristics of Magnetic Composite Material Composed with Gd and $Gd_{1-x}Ho_x$ Alloy

Zhichao Xu[1] · Fupeng Wang[2] · Guoxing Lin[3]

Received: 26 July 2020 / Accepted: 20 October 2020 / Published online: 28 October 2020

Abstract

The doping of Ho into Gd can not only adjust the Curie temperature of $Gd_{1-x}Ho_x$ alloy but also enhance the maximal magnetic entropy change. In the present paper, the magnetocaloric characteristics of $Gd_{1-x}Ho_x$ alloys were calculated by means of the de Gennes model, and the isothermal magnetic entropy change of $Gd_{1-x}Ho_x$ ($x = 0, 0.05, 0.10, 0.15, 0.20$) alloys versus temperature curves generally exhibit a caret-like shape. Furthermore, the composite material composed of Gd and $Gd_{0.80}Ho_{0.20}$ is introduced in order to obtain a gentler entropy change curve over a large temperature span. Consequently, it is found under magnetic field change from 0 to 2 T that the composite composed of Gd and $Gd_{0.80}Ho_{0.20}$ with 67% mass ratio of Gd possesses a maximal full width at half maxima δT_{FWHM} of the isothermal magnetic entropy change curve which is 87.3 K, with temperature 217.9 K of the cold end at half-width and temperature 305.2 K of the hot end at half-width. In such a case, the maximal magnetic entropy change is 4.17 J/(kgK), relative cooling power *(RCP)* is about 360 J/kg, and refrigeration capacity (*RC*) achieves 280.6 J/kg. The results show that the composite magnetocaloric material can largely enhance the material performance for magnetic refrigeration application.

Keywords Magnetocaloric material · Composite · Relative cooling power · Refrigeration capacity

1 Introduction

Magnetocaloric effect (MCE) arises from the entropy change of magnetocaloric materials (MCMs) due to magnetic field variation [1–4]. Because MCMs are generally solid and compact, such that magnetic refrigeration technology based on MCMs presents no Global Warming Potential (GWP) or Ozone Depletion Potential (ODP). For this reason, MCMs have been extensively explored for its potential application in the room temperature (RT) magnetic refrigeration [5, 6].

Magnetocaloric refrigeration material gadolinium (Gd) [7] as the working substance was used in RT magnetic refrigeration experimental machine in 1976. Afterward, a variety of magnetocaloric materials with a large magnetocaloric effect have been found and explored, such as $Gd_5Si_2Ge_2$ [7], $MnFeP_{0.45}As_{0.5}$ [8], $LaFe_{11.4}Si_{1.6}$ [9], and $La_{1-x}Ca_xMnO_3$ ($x = 0.2, 0.33$) [10]. However, only under 5 T external magnetic field change can these materials be magnetized saturatedly, stimulating a lattice structural transition and resulting in a giant magnetocaloric effect (GMCE), named first-order transition (FOT) material [11]. However, the temperature region where the large magnetic entropy changes occurs in a narrow temperature range. On the other hand, some magnetocaloric materials only exhibit ferromagnetic-paramagnetic phase transition [12, 13], named second-order transition (SOT) material. Compared with the FOT materials, the entropy change of SOT materials is lower, but it does not possess thermal hysteresis and magnetic hysteresis [14]. Therefore, there were some scholars and engineers paying more attention to searching for SOT materials with large magnetic entropy change [15, 16].

✉ Zhichao Xu
xu-zhichao@163.com

✉ Guoxing Lin
gxlin@xmu.edu.cn

[1] Ministry of Education's Key Laboratory of Poyang Lake Wetland and Watershed Research, Jiangxi Normal University, Nanchang 330022, China

[2] Department of Fashion Communication and Media, Jiangxi Institute of Fashion Technology, Nanchang 330201, China

[3] College of Physical Science and Technology, Xiamen University, Xiamen 361005, China

Among the SOT materials, Gd, whose Curie temperature is 293 K, was considered to be an ideal working substance for RT magnetic refrigerant and has been efficiently utilized in current prototypes [17]. Furthermore, Gd-based rare earth alloys such as gadolinium-terbium (Gd-Tb), gadolinium-holmium (Gd-Ho), gadolinium-dysprosium (Gd-Dy), and gadolinium-erbium (Gd-Er) can be used as the RT magnetic refrigerant due to enhanced MCE and the adjustable Curie temperature around RT [18, 19]. Balli et al. [18] and Hou et al. [17] separately found that the doping of Tb and Dy into Gd can adjust the Curie temperature of Gd, where $Gd_{0.7}Tb_{0.3}$ and $Gd_{0.73}Dy_{0.27}$ can reach a maximal entropy change of 10.2 J/(kgK) under 5 T field variation and adiabatic temperature change of 3.1 K at 260 K under 1.2 T field variation. However, these Gd-based rare earth materials generally exhibit a caret-like entropy curve as temperature, and it is conflicting with that a perfect Ericsson refrigeration cycle requires a constant isothermal entropy change of the working substance over operating temperature region [14]. Thus, in order to obtain a relatively gentle entropy change curve of magnetocaloric material, some researchers focused their attentions on the study of the magnetocaloric effect of composite. For example, Bao et al. [20] found that the composite material composed with $Gd_{50}Al_{30}Co_{20}$ and $Gd_{55}Al_{20}Co_{25}$ can obtain nearly a constant entropy change 8.69 J/(kgK) under 5 T field variation. Ma et al. [21] found that a composite, composed of $Gd_{50}Co_{48}Fe_2$ and $Gd_{50}Co_{48}Mn_2$ with a mass ratio of 7:3, could reach 4.32 J/(kgK) isothermal entropy change between 255 K and 275 K under 5 T field variation. Zhong et al. [22] found that the multilayer composite composed of $Gd_{65}Mn_{25}Si_{10}$ and Gd (mass ratio of 7:3) exhibits a large MCE with enhanced δT_{FWHM} 212 K of the isothermal magnetic entropy change curve as well as large *RC* of 724 J/kg under 5 T field variation. Xu et al. [23] investigated that the composite, composed of Gd, $Gd_{0.91}Ho_{0.09}$ and $Gd_{0.8}Ho_{0.2}$ with a mass ratio of 0.59:0.17:0.24, can obtain a nearly constant magnetic entropy change of 4.09 J/(kgK) and found that the regenerative Ericsson refrigeration cycle using the composite material composed with Gd-Ho alloy exhibits a better performance than that of the component materials.

The composite material possesses a gentler isothermal entropy change curve than the component materials. But we also need some other parameters to evaluate the MCE and refrigeration performance of composite material. Therefore, the *RC* and *RCP* are introduced to compare the magnetic material, including the composite. In this paper, we analyzed the magnetocaloric characteristics including the maximal entropy change, full width at half maximum of the isothermal entropy change curve (δT_{FWHM}), *RCP* and *RC* of $Gd_{1-x}Ho_x$ ($x = 0$, 0.05, 0.10, 0.15, 0.20), as well as the composite composed with Gd and $Gd_{0.80}Ho_{0.20}$ alloy. The results obtained can provide some references for the selection and parametric design of RT magnetic refrigeration materials.

2 Thermodynamic Analysis of Materials

2.1 Thermodynamic Analysis of Single Element Magnetocaloric Material

First of all, considering a single element ferromagnetic material, its magnetic entropy $S(H, T)$ can be written as [24]

$$S(H,T) = R\left\{\ln\left[\frac{\sinh[y(2J+1)/2J]}{\sinh(y/2J)}\right] - yB_J(y)\right\} \tag{1}$$

where R and J are universal gas constant and angular quantum number, respectively, and $B_J(y) = \coth[y(2J+1)/2J](2J+1)/2J - (1/2J)\coth(y/2J)$ is the Brillouin function. Additionally, y can be obtained from the state equation of ferromagnetic material, i.e.,

$$M = NgJ\mu_B B_J(y) \tag{2}$$

$$y = g\mu_B\mu_0 J(H + \lambda M)/kT \tag{3}$$

where N is the number of magneton per unit volume, g is the Lander factor, μ_B is the Bohr magneton, μ_0 is the vacuum permeability, H ($B = \mu_0 H$) is the external magnetic field, λ is the molecular field coefficient, k is the Boltzmann constant, and T is the absolute temperature. For the given external magnetic field and temperature, the magnetization M and y can be solved out through Eqs. (2) and (3). Subsequently, according to Eq. (1), the magnetic entropy can be calculated.

2.2 De Gennes Factor Model Applying to Binary Alloys

Note that Eqs. (1), (2), and (3) can be used to calculate the magnetic entropy of single element ferromagnetic material. For binary alloys $Gd_{1-x}Ho_x$, we may employ the de Gennes factor model method. The expressions of the de Gennes factors and the effective magnetic moment for the alloy $Gd_{1-x}Ho_x$ are given by [25].

$$\overline{G} = \left(\overline{g}-1\right)^2\overline{J}\left(\overline{J}+1\right) = (1-x)G_{Gd} + xG_{Ho} \tag{4}$$

$$\overline{\mu}^2 = \overline{g}^2\overline{J}\left(\overline{J}+1\right)\mu_B^2 = (1-x)\mu_{Gd}^2 + x\mu_{Ho}^2 \tag{5}$$

where $\overline{g}$ is the effective Lander factor; $\overline{J}$ the effective angular moment number; x is the molar fraction of Ho in the alloy $Gd_{1-x}Ho_x$; G_{Gd} and G_{Ho} are the de Gennes factors; and μ_{Gd} and μ_{Ho} are the effective magnetic moments of Gd and Ho material, respectively, and $G_{Gd/Ho}$ and $\mu_{Gd/Ho}$ can be calculated through Eqs. (6) and (7):

$$G_{Gd/Ho} = \left(g_{Gd/Ho}-1\right)^2 J_{Gd/Ho}\left(J_{Gd/Ho}+1\right) \tag{6}$$

$$\mu_{Gd/Ho} = g_{Gd/Ho}\sqrt{J_{Gd/Ho}\left(J_{Gd/Ho}+1\right)}\mu_B \tag{7}$$

where $g_{Gd/Ho}$ and $J_{Gd/Ho}$ are the Lander factor and angular quantum number of Gd/Ho. Based on Eqs. (4), (5), (6), and (7) and the relevant data of Gd and Ho listed in Table 1, $\overline{g}$, $\overline{J}$, and $\overline{G}$ as well as $\overline{\mu}$ can be obtained. On the other hand, the Curie temperature T_c of $Gd_{1-x}Ho_x$ alloy can be calculated from the following equation [27]:

$$T_c = 46.63\overline{G}^{2/3} \tag{8}$$

3 Relative Cooling Power and Refrigeration Capacity

Using the Lander factor and angular quantum number of $Gd_{1-x}Ho_x$ alloy, the magnetic entropy of $Gd_{1-x}Ho_x$ can be calculated by using Eqs. (1), (2), and (3). Furthermore, for a given magnetic field or field variation, the isothermal magnetic entropy change curve of $Gd_{1-x}Ho_x$ as well as the δT_{FWHM} can be obtained. In order to compare the refrigeration performance of the magnetocaloric materials, there are two parameters; the relative cooling power (*RCP*) and refrigeration capacity (*RC*) [28–31] should be adopted. The *RCP* is defined as the product of $(-\Delta S_{max})$ and δT_{FWHM} of the isothermal magnetic entropy change curve, that is,

$$RCP = -\Delta S_{\max} \times \delta T_{FWHM} \tag{9}$$

while *RC* is determined as

$$RC = \int_{T_{r2}}^{T_{r1}} -\Delta S(\Delta B, T)dT \tag{10}$$

where T_{r1} and T_{r2} are the temperatures of the cold and the hot end at half height of maximal entropy change curve respectively.

4 Results and Discussion

4.1 The MCE Characteristics of $Gd_{1-x}Ho_x$ Alloys

Magnetic materials, due to their space lattice and electron motion differences, may be classified as diamagnetic, paramagnetic, ferromagnetic, antiferromagnetic, and ferrimagnetic ones. For room temperature magnetic refrigeration, MCE properties of ferromagnetic and paramagnetic materials are often utilized. It is well known that Gd material shows a paramagnetic to ferromagnetic transition when the temperature decreases or an external magnetic field is applied. Similarly, the $Gd_{1-x}Ho_x$ also experiences the same magnetic phase transition when Ho concentration is lower than 0.25 [32]. However, though the doping of Ho does not change the magnetic material phase transition category fundamentally, it can influence the magnetic material properties such as angular moment number, Lander factor, consequently the magnetocaloric properties such as Curie temperature, magnetic entropy change, and so on. Based on the relevant data of Gd and Ho in Table 1, the effective Lander factor, effective angular moment number, and Curie temperature of $Gd_{1-x}Ho_x$ ($x = 0$, 0.05, 0.10, 0.15, 0.20) can be obtained by using de Gennes factor model method. Subsequently, the theoretical isothermal entropy change of $Gd_{1-x}Ho_x$ ($x = 0$, 0.05, 0.10, 0.15, 0.20) curves as temperature under 0 to 2 T field variation are obtained, as shown in Fig. 1a. And Fig. 1b shows the comparison between the experimental data [33] and the theoretical entropy change of $Gd_{0.80}Ho_{0.20}$. Figure 1b indicates that the experimental entropy change of $Gd_{0.80}Ho_{0.20}$ under 1 T field variation fits well enough with the theoretical ones, which is good support of the de Gennes method used in this paper. Moreover, it also can be clearly seen that the isothermal entropy change curves of $Gd_{1-x}Ho_x$ alloys ($x = 0$, 0.05, 0.10, 0.15, 0.20) versus temperature all exhibit a caret-like shape curve. Furthermore, as Ho concentration increases, the Curie temperatures of $Gd_{1-x}Ho_x$ ($x = 0$, 0.05, 0.10, 0.15, 0.20) are 293 K, 286 K, 278.9 K, 271.7 K, and 264.4 K, and maximal isothermal entropy variations are 5.63 J/(kgK), 5.78 J/(kgK), 5.94 J/(kgK), 6.11 J/(kgK), and 6.29 J/(kgK) under 2 T field variation, respectively. Additionally, it can be seen in Table 2 that both *RCP* and *RC* of $Gd_{1-x}Ho_x$ increase with Ho concentration, where the δT_{FWHM} approximately keeps constant, about 47 K, and T_{r1} and T_{r2} shift to low temperature region.

4.2 The MCE and Refrigeration Characteristics of the Composite

Notice that the alloys $Gd_{1-x}Ho_x$ ($x = 0$, 0.05, 0.10, 0.15, 0.20) exhibit a caret-like entropy change curve, resulting in a relatively low cooling power, especially when the operating temperatures of the working temperature deviate from the transition temperature. Thus, it is important to prepare the composite with Gd and $Gd_{1-x}Ho_x$ undergoing successive transition temperatures [34–36], where the composite owns two Curie

Table 1 Relevant parameter values of Gd and Ho [26]

Material	Lander factor	Angular quantum number	Density (kg/m^3)	Molar mass (kg/mol)
Gd	2	3.5	7901	0.157
Ho	1.25	8	8795	0.165

Table 2 The MCE and refrigeration characteristics of Gd and $Gd_{1-x}Ho_x$ alloys under applied magnetic field variation from 0 to 2 T

	T_c (K)	$-\Delta S_{max}$ (J/(kgK))	T_{r1} (K)	T_{r2} (K)	δT_{FWHM} (K)	*RCP* (J/kg)	*RC* (J/kg)
Gd	293.0	5.63	257.5	305.1	47.6	267.9	188.9
$Gd_{0.95}Ho_{0.05}$	286.0	5.78	250.4	298.2	47.8	276.4	194.9
$Gd_{0.90}Ho_{0.10}$	278.9	5.94	243.4	291.1	47.7	283.5	200.1
$Gd_{0.85}Ho_{0.15}$	271.7	6.11	236.3	283.9	47.6	290.9	205.4
$Gd_{0.80}Ho_{0.20}$	264.4	6.29	229.2	276.7	47.5	298.5	210.7

temperatures and the entropy change curves exhibit two peaks which are located at the Curie temperatures of the two component materials, respectively. The composite material generally exhibits a gentler and large magnetic entropy change over a wide temperature region such that the δT_{FWHM} as well as the *RC* and *RCP* will be enhanced. For this reason, we design and establish one new composite material composed with Gd and $Gd_{0.80}Ho_{0.20}$, The isothermal magnetic entropy change with different Gd mass ratios y in the composite are to be analyzed and discussed. Subsequently, the isothermal magnetic entropy change curves of the composite with different y (0.20, 0.40, 0.60, 0.67, 0.80) are obtained under 2 T field variation, as shown in Fig. 2. It is found that the optimized mass ratio y_{opt} of Gd is equal to 0.67 by using the optimization method which is based on the following equations [23]:

$$-\Delta S_{com}\left(\Delta B, T_{c,Gd}\right) = -\Delta S_{com}\left(\Delta B, T_{c,Gd_{0.80}Ho_{0.20}}\right) \tag{11}$$

$$-\Delta S_{com}\left(\Delta B, T_{c,Gd}\right) = y\left[-\Delta S_{Gd}\left(\Delta B, T_{c,Gd}\right)\right] + (1-y)\left[-\Delta S_{Gd_{0.80}Ho_{0.20}}\left(\Delta B, T_{c,Gd}\right)\right] \tag{12}$$

$$-\Delta S_{com}\left(\Delta B, T_{c,Gd_{0.80}Ho_{0.20}}\right) = y\left[-\Delta S_{\mathrm{Gd}}\left(\Delta B, T_{c,Gd_{0.80}Ho_{0.20}}\right)\right] + (1-y)\left[-\Delta S_{Gd_{0.80}Ho_{0.20}}\left(\Delta B, T_{c,Gd_{0.80}Ho_{0.20}}\right)\right] \tag{13}$$

where the entropy change of Gd and $Gd_{0.80}Ho_{0.20}$ is listed in Table 3.

It can be clearly seen from Fig. 2 that the isothermal entropy change curve of the composite with the optimized mass ratio of Gd is most gentle than that of the composites with other Gd mass ratios, where the maximal entropy change and δT_{FWHM} reach 4.17 J/(kgK) and 87.3 K. Furthermore, the influence of Gd mass ratio y on the MCE and refrigeration characteristics of the composite including ΔS_{max}, δT_{FWHM}, *RCP*, *RC*, T_{r1}, and T_{r2} can be evaluated and discussed on the basis of Fig. 3. From Fig. 3a, one can see that T_{r2} increases to a constant 305.2 K when $y > 0.67$. There is a region with rapid increased slope of T_{r2} around $y = 0.33$. On the other hand, Fig. 3a shows that T_{r1} firstly decreases and then increases with increasing Gd material mass ratio; its minimal value is 217.9 K when $y = 0.67$. Accordingly, when $y = 0.67$, δT_{FWHM} of the composite material achieves its maximal value

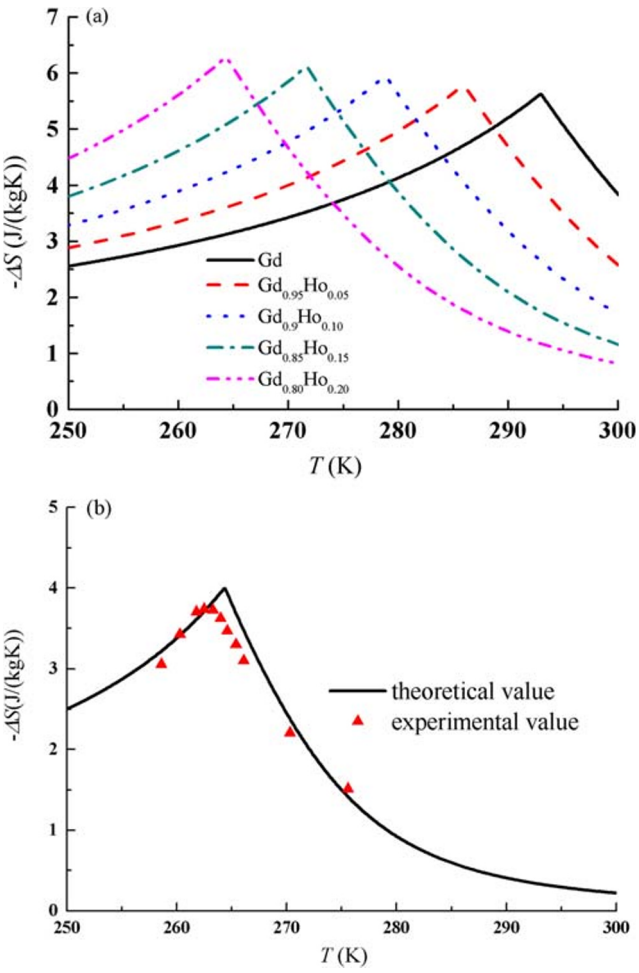

Fig. 1 **a** The theoretical isothermal entropy change versus temperature curves of $Gd_{1-x}Ho_x$ ($x = 0, 0.05, 0.10, 0.15, 0.20$) under applied magnetic field variation from 0 to 2 T. **b** The experimental [33] and theoretical entropy change of $Gd_{0.80}Ho_{0.20}$ under 1 T field change

Table 3 The isothermal entropy change values of Gd and $Gd_{0.80}Ho_{0.20}$ at their respective Curie temperature (264.4 K and 293.0 K) under 2 T magnetic field variation

T_c	264.4 (K)	293.0 (K)
Gd	3.13 J/(kgK)	5.63 J/(kgK)
$Gd_{0.80}Ho_{0.20}$	6.29 J/(kgK)	1.18 J/(kgK)

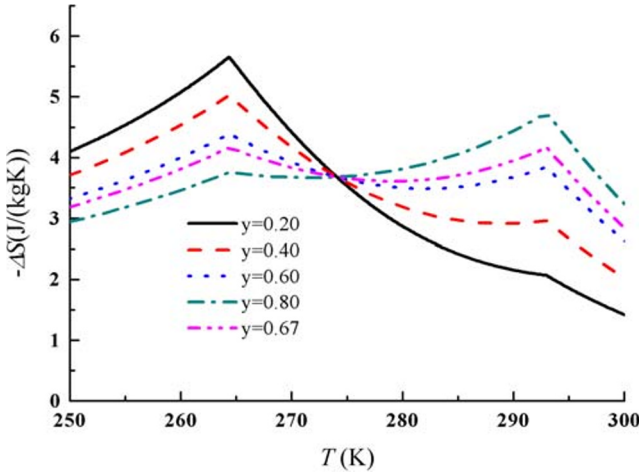

Fig. 2 The magnetic entropy change versus temperature curves of the composite with Gd and $Gd_{0.80}Ho_{0.20}$, where y denotes the mass ratio of Gd in the composite as well as 2 T applied magnetic field variation

of 87.3 K, which is coincident with the optimized Gd material mass ratio calculated theoretically above. Additionally, it can be seen in Fig. 3b that the maximal entropy change exhibits a V-shaped curve with a minimal value 4.17 J/(kgK), while *RC* achieves a maximal value 280.6 J/kg when $y = 0.67$ and *RCP*

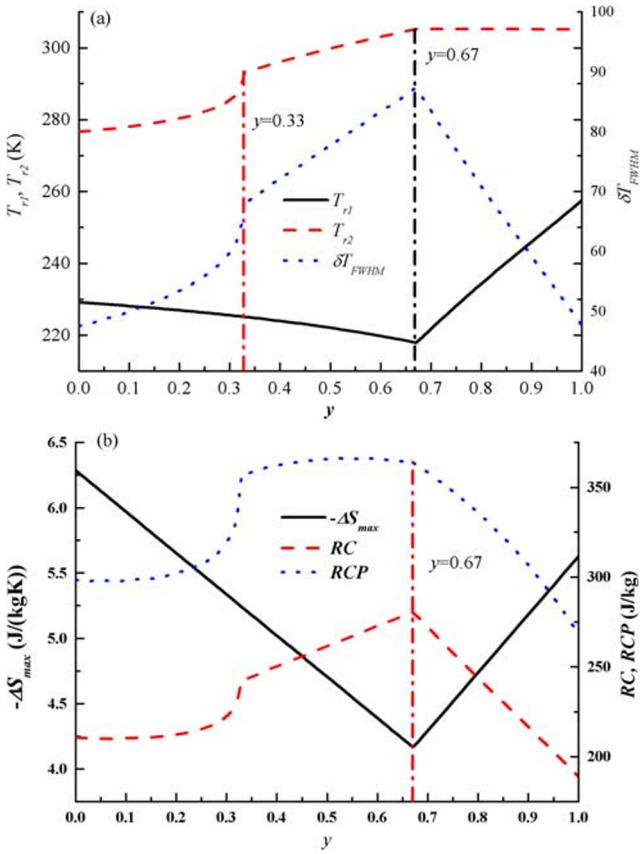

Fig. 3 The $T_{r,}$ $T_{r2,}$ δT_{FWHM}, maximal isothermal entropy change, and *RC* and *RCP* curves versus Gd mass ratio y in the composite under applied field variation from 0 to 2 T

curve exhibits a plateau, 360 J/kg or so, when y is between 0.33 and 0.67.

In Fig. 1, it can be seen clearly that the Curie temperature of $Gd_{1-x}Ho_x$ decreases while the maximal entropy change increases with increasing Ho concentration in $Gd_{1-x}Ho_x$ alloy. This means that the doping of Ho into Gd not only can adjust the Curie temperature but also can enhance the MCE of material. This is also matched with the following equation [37, 38]:

$$\Delta S_{\max} = -1.07qR\left(\frac{g\mu_B JH}{kT_c}\right)^{2/3} \tag{14}$$

where q is the number of magnetic ions and there is an inverse correlation between Curie temperature and the maximal entropy change of alloys. The decrease of material Curie temperature will lead to shifting T_{r1} and T_{r2} to lower temperature with a constant δT_{FWHM}, and both *RCP* and *RC* increase with enhanced material entropy change, which can be found in Table 2.

In Fig. 2, the entropy change curves of the composite are gentler than that of single component material shown in Fig. 1. It can be ascribed by the fact that the entropy change of the composite equals the linear combination of the component material entropy change. Additionally, the component Gd-Ho alloy has only one entropy change peak at its Curie temperature, but the composite material owns more than one entropy change peak, whose number depends on the component material number. Moreover, the maximal entropy change of the composite will decrease to a certain extent, but it can enhance largely the δT_{FWHM}, as seen in Table 4. This may be also explained as follows: The entropy change of the composite results from the linear combination of the component material entropy changes, that is,

$$-\Delta S_{com}(\Delta B, T) = [-\Delta S_{Gd}(\Delta B, T)]y + [-\Delta S_{Gd_{0.80}Ho_{0.20}}(\Delta B, T)](1-y) \tag{15}$$

By integrating Eq. (15), it yields

$$\int_0^\infty -\Delta S_{com}(\Delta B, T)dT = \int_0^\infty -\Delta S_{Gd_{0.80}Ho_{0.20}}(\Delta B, T)dT + y\int_0^\infty \left\{[-\Delta S_{Gd}(\Delta B, T)] - \left[-\Delta S_{Gd_{0.80}Ho_{0.20}}\left(\Delta B, T\right)\right]\right\}dT \tag{16}$$

In the case, one can see from Fig. 1 that the value of $-\Delta S_{Gd}(\Delta B,T)$ is larger/smaller than those of $-\Delta S_{Gd_{0.80}Ho_{0.20}}(\Delta B,T)$ when the temperature is larger/smaller than 275 K. And both $-\Delta S_{Gd}(\Delta B,T)$ and $-\Delta S_{Gd_{0.80}Ho_{0.20}}(\Delta B,T)$ approximately equal zero at ultra-high and low temperatures. Consequently, $\int_0^\infty \{[-\Delta S_{Gd}(\Delta B, T)] - [-\Delta S_{Gd_{0.80}}\ Ho_{0.20}(\Delta B, T)]\}$ dT can be thought as a tiny value, and the $\int_0^\infty -\Delta S_{com}(\Delta B, T)$ dT can be approximately thought as a constant. Thus, when the

Table 4 The MCE and refrigeration characteristics of the composite composed with Gd and $Gd_{0.80}Ho_{0.20}$ under 2 T applied magnetic field variation

	$-\Delta S_{max}$ J/(kgK)	T_{r1} (K)	T_{r2} (K)	δT_{FWHM} (K)	*RCP* (J/kg)	*RC* (J/kg)	*RC*/*RCP*
$y = 0.20$	5.65	227.0	280.4	53.4	301.9	212.3	0.703
$y = 0.40$	5.02	224.0	296.1	72.1	362.0	250.3	0.691
$y = 0.60$	4.39	219.8	303.1	83.3	365.6	272.8	0.746
$y = 0.67$	4.17	217.9	305.2	87.3	363.6	280.6	0.772
$y = 0.80$	4.74	234.3	305.2	70.9	335.9	244.0	0.726

maximal entropy change decreases, the δT_{FWHM} generally increases to some extent.

In Fig. 3a, one can see that the slope of T_{r2} curve increases when $y = 0.33$. It can be explained in Fig. 4, where the entropy change of the composite at 264.4 K is equal to 5.24 J/(kgK) which is approximately twice of that at 293.2 K. This indicates that the temperature T_{r2} changes dramatically when y is equal to 0.33. Furthermore, the δT_{FWHM} of entropy change curve of Gd-Ho alloy reaches the largest value when Gd mass ratio equals to 0.67, which is consistent with the value 0.67 shown in Fig. 2. It means that the calculation method of the optimal mass ratio can optimize not only the component material mass ratio to get a gentler entropy change curve of the composite but the δT_{FWHM} related to *RC* and *RCP* indirectly.

There is a difference in Fig. 3b that the *RCP* exhibits a plateau while *RC* exhibits an obvious maximum. It can be explained with the definition of the related parameters. The *RCP* is determined by the maximal entropy change and the δT_{FWHM} in the entropy change curve, while *RC* depends on the δT_{FWHM} and the entropy change within the temperature region of the δT_{FWHM}. Generally the value of *RCP* is larger than that of *RC*, and the values are the same if the entropy change curve would be absolutely flat from T_{r1} to T_{r2}. Therefore, the ratio of *RC* to *RCP* can stand for the gentle degree of the related entropy change curve. The larger the ratio, the gentler the related entropy change curve is. For example, one can see from Fig. 3b that when y equals to 0.67, or the value of *RC*/*RCP* is equal to 0.772 shown in Table 4, the composite material entropy curve is gentlest.

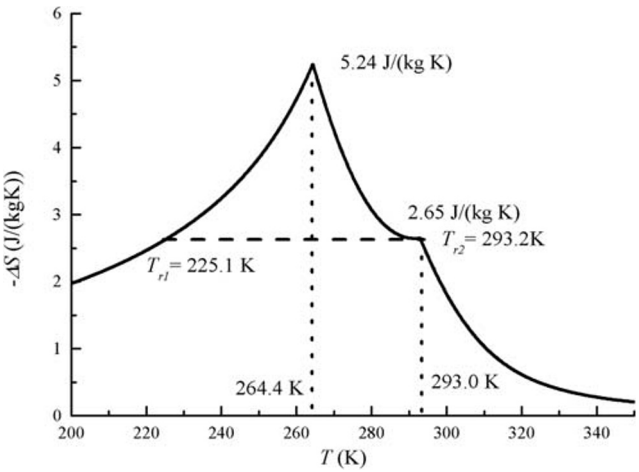

Fig. 4 The magnetic entropy change curve of the composite composed with Gd and $Gd_{0.80}Ho_{0.20}$, where Gd mass ratio is 0.33

5 Conclusions

Based on the de Gennes factor model method, the MCE of Gd, $Gd_{1-x}Ho_x$ ($x = 0$, 0.05, 0.10, 0.15, 0.20), and the composite composed with Gd and $Gd_{0.80}Ho_{0.20}$ are investigated numerically. It is found that the composite composed of Gd and $Gd_{0.80}Ho_{0.20}$ with the mass ratio of 0.67:0.33 can reach the most perfect entropy change curve, with a maximal entropy change of 4.17 J/(kgK) and δT_{FWHM} of 87.3 K, where Tr_1 and Tr_2 are 217.9 K and 305.2 K respectively under applied magnetic field varying from 0 to 2 T. Simultaneously, *RC* of the composite reaches the maximum value, 280.6 J/kg, when Gd mass ratio is 0.67, and *RCP* reaches a plateau, about 360 J/kg, when Gd mass ratio is between 0.33 and 0.67, under 2 T field change.

Acknowledgements This work was supported by the Opening Fund of Key Laboratory of Poyang Lake Wetland and Watershed Research (Jiangxi Normal University), Ministry of Education (No. PK2017006), and the National Natural Science Foundation (No. 51776178), People's Republic of China.

Compliance with Ethical Standards

Conflict of Interest The authors declare that they have no conflict of interest.

References

1. Guedri, A.: Sintering temperature effects on structural, magnetic, magnetocaloric and critical properties of $Nd_{0.67}Pb_{0.33}Mn_{0.9}Al_{0.1}O_3$ manganites. J. Supercond. Nov. Magn. **33**, 1223 (2020)
2. Yang, Z.X.: Magnetism and magnetocaloric effects of R_3Pd_4 (R = Nd and Pr) compounds. J. Supercond. Nov. Magn. **33**, 1851 (2020)
3. Zhang, H.H.: Increasing working temperature span in Ni-Mn-Sn-Co alloys via introducing pores. J. Magn. Magn. Mater. **500**, 166359 (2020)

4. Shang, Y.F.: Structure, magnetic properties, and magnetocaloric effect of polycrystalline Ho_3M (M = Rh, Ru) alloys. J. Magn. Magn. Mater. **497**, 166055 (2020)
5. Franco, V.: The magnetocaloric effect and magnetic refrigeration near room temperature: materials and models. Annu. Rev. Mater. Res. **42**, 305 (2012)
6. Yu, B.F.: Review on research of room temperature magnetic refrigeration. Int. J. Refrig. **26**, 622 (2003)
7. Pecharsky, V.K.: Giant magnetocaloric effect in $Gd_5(Si_2Ge_2)$. Phys. Rev. Lett. **78**, 4494 (1997)
8. Tegus, O.: Transition-metal-based magnetic refrigerants for room-temperature applications. Nature. **415**, 150 (2002)
9. Hu, F.X.: Influence of negative lattice expansion and metamagnetic transition on magnetic entropy change in the compound $LaFe_{11.4}Si_{1.6}$. Appl. Phys. Lett. **78**, 3675 (2001)
10. Guo, Z.B.: Large magnetic entropy change in perovskite-type manganese oxides. Phys. Rev. Lett. **78**, 1142 (1997)
11. Castañeda, E.J.G.: Effect of quenching and normalizing on the microstructure and magnetocaloric effect of a Cu–11Al–9Zn Alloy with 6.5 wt % Ni–2.5 wt % Fe. Magnetochemistry **5**, 48 (2019)
12. Zheng, X.Q.: Research progress in magnetocaloric effect materials. Acta Phys. Sin. **65**, 217502 (2016)
13. Gómez, J.R.: A review of the thermodynamic cycles in magnetic refrigeration. Renew. Sust. Energ. Rev. **17**, 74 (2013)
14. Franco, V.: Magnetocaloric effect: from materials research to refrigeration devices. Prog. Mater. Sci. **93**, 112 (2018)
15. Issaoui, F.: Theoretical insights into the stability of perovskite clusters by studying magnetization and magnetocaloric effect of $Nd_{0.6}Sr_{0.4}MnO_3$ compound at room temperature. J. Low. Temp. Phys. **200**, 1 (2020)
16. Chouikhi, S.: Modeling of magnetic, magnetocaloric properties and dielectrical characterization of $(La_{0.75}Nd_{0.25})_{2/3}(Ca_{0.8}Sr_{0.2})_{1/3}MnO_3$ manganite oxide. J. Low. Temp. Phys. **197**, 471 (2019)
17. Yang, Z.M.: Thermoeconomic performance optimization of an irreversible Brayton refrigeration cycle using Gd, $Gd_{0.95}Dy_{0.05}$ or $Gd_{0.95}Er_{0.05}$ as the working substance. J. Magn. Magn. Mater. **499**, 166189 (2020)
18. Balli, M.: $Gd_{1-x}Tb_x$ alloys for Ericsson-like magnetic refrigeration cycles. J. Alloys Compd. **442**, 129 (2007)
19. Hou, X.L.: Research for magnetocaloric effect of $Gd_{1-x}Dy_x$ alloy. Phys. Status Solidi C. **4**, (2007)
20. Bao, Y.: Table-like magnetocaloric behavior and enhanced cooling efficiency of a Bi-constituent Gd alloy wire-based composite. J. Alloys Compd. **764**, 789 (2018)
21. Ma, L.Y.: Achieving a table-like magnetic entropy change across the ice point of water with tailorable temperature range in Gd-Co-based amorphous hybrids. J. Alloys Compd. **723**, 197 (2017)
22. Zhong, X.C.: Table-like magnetocaloric effect and large refrigerant capacity in $Gd_{65}Mn_{25}Si_{10}$-Gd composite materials for near room temperature refrigeration. Today Commun. **14**, 22 (2018)
23. Xu, Z.C.: A Gd_xHo_{1-x}-based composite and its performance characteristics in a regenerative Ericsson refrigeration cycle. J. Alloys Compd. **520**, 639 (2015)
24. Diguet, G.: Effect of geometrical shape of the working substance gadolinium on the performance of a regenerative magnetic Brayton refrigeration cycle. J. Magn. Magn. Mater. **326**, 103 (2013)
25. Aprea, C.: Modelling an active magnetic refrigeration system: a comparison with different models of incompressible flow through a packed bed. Appl. Therm. Eng. **36**, 296 (2012)
26. Buschow, K.H.J.: Boer. F.: Physics of magnetism and magnetic materials. Kluwer. N. Y. (2003)
27. Hsieh, C.M.: Modeling of graded active magnetic regenerator for room-temperature. IEEE Trans. Magn. **50**, 4002904 (2014)
28. Lyubina, J.: Magnetocaloric materials for energy efficient cooling. J. Phys. D. Appl. Phys. **50**, 053002 (2017)
29. Li, L.W.: Recent progresses in exploring the rare earth based intermetallic compounds for cryogenic magnetic refrigeration. J. Alloys Compd. **823**, 153810 (2020)
30. Katagiri, K.: Magnetocaloric properties and magnetic refrigerant capacity of $MnFeP_{1-x}Si_x$. J. Alloys Compd. **553**, 286 (2013)
31. Jeddi, M.: Phenomenological modeling of magnetocaloric properties in $0.75La_{0.6}Ca_{0.4}MnO_3/0.25La_{0.6}Sr_{0.4}MnO_3$ nanocomposite manganite. J. Low. Temp. Phys. **198**, 135 (2020)
32. Fujii, H.: Magnetic anisotropy in the binary alloys of Gd with the other heavy rare earth metals. J. Phys. Soc. Jpn. **41**, 1179 (1976)
33. Tishin, A.M.: Working substances for magnetic refrigerators. Cryogenics. **30**, 720 (1990)
34. Shen, H.X.: The magnetocaloric composite designed by multi-Gd-Al-Co microwires with close performances. Phys. Stat. Sol. (A). **216**, 1900090 (2019)
35. Diguet, G.: Performance characteristics of a regeneration Ericsson refrigeration cycle using a magnetic composite as the working substance. Int. J. Refrig. **36**, 958 (2013)
36. Synoradzki, K.: Magnetocaloric effect in $Gd_5(Si,Ge)_4$ based alloys and composites. J. Rare Earths. **37**, 1218 (2019)
37. Gschneidner Jr., K.A.: Magnetocaloric materials. Annu. Rev. Mater. Sci. **30**, 387 (2000)
38. Zhu, R.W.: Magnetocaloric effect in co-based amorphous alloy $Co_{90}Nb_{10}Ta_3$. J. Magn. Magn. Mater. **484**, 253 (2019)